EDUCE WP 1.4 - RAFs for ozone and albedo
by Antti Arola
Finnish Meteorological Institute

1. Introduction

This report describes the work carried out in the WP1.4, titled "RAFs for ozone and albedo". The work reported here is mostly concentrated on the effect of snow albedo in surface UV, since ozone RAF (*Madronich* [1993]) is well defined and several studies have added into our knowledge on the effects of ozone (*WMO* [2002]). However, an attempt was made to estimate the ozone dependent ozone RAF, as discussed below.

2. Ozone RAF

Ozone RAF is mostly a function of ozone and solar zenith angle (sza), although often a single value is assumed, for instance 1 or 1.1 for CIE dose rates. Figure 1 shows the model derived ozone RAF against sza for several ozone amounts. In y-axis is the ozone RAF, calculated by using the power law form. It can be noted that for the sza values of less than 50 degrees, 1.1 is a reasonable estimate. However, for the larger values RAF decreases rather rapidly with both sza and ozone. These dependencies are important, particularly in locations with large sza values, such as in Arctic.

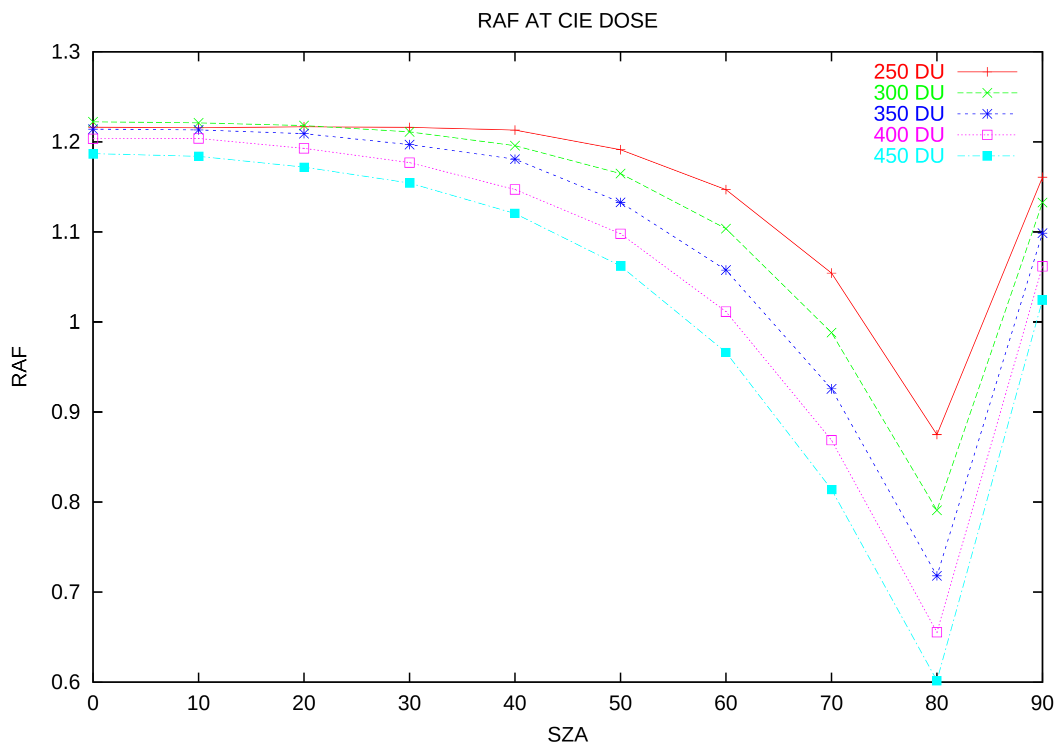

Figure 1. The ozone RAF of CIE dose rate as a function of ozone and sza.

Figure 2 shows otherwise identical simulation, but for a single wavelength of 305 nm. Again, the dependency on sza and ozone is apparent. While a constant ozone RAF is often assumed, in some studies the sza dependency have been taken into account, when it has been estimated at some particular wavelength using measurements at selected sza (e.g. *Bais et al.* [1993], *Fioletov et al.* [1997]). Ozone dependency can be readily estimated through the radiative transfer modeling. However, it is not as straight-forward task to perform from the spectral measurements and, to our knowledge, has not been attempted to carry out. In this WP, the feasibility of this kind of approach was tested.

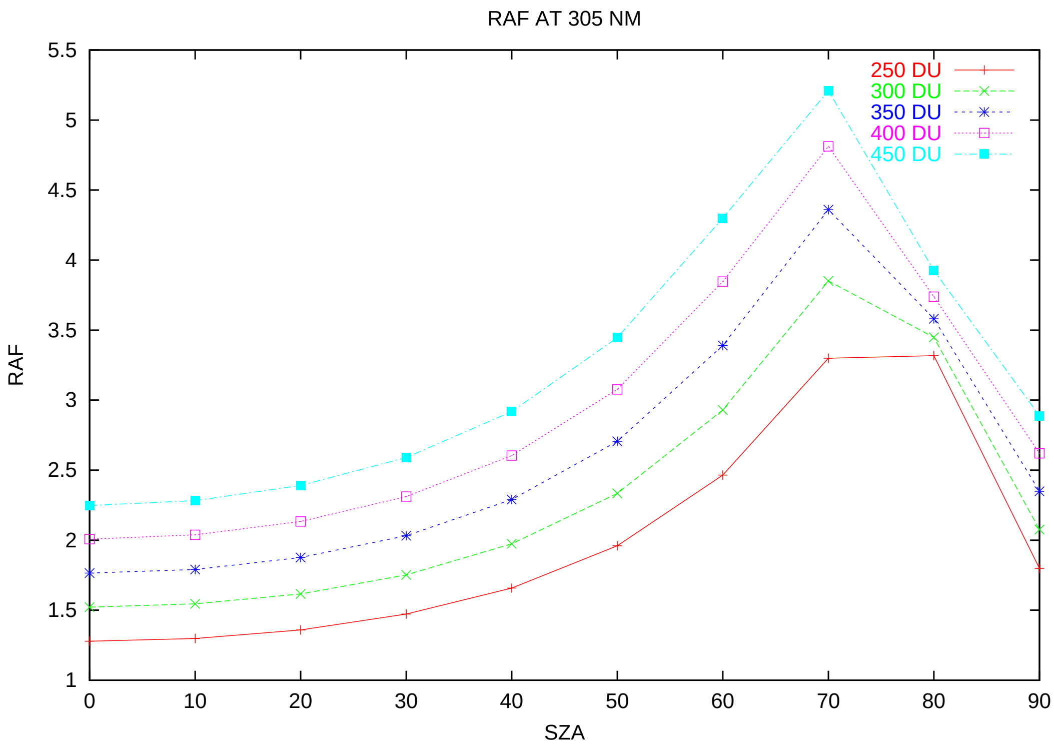

Figure 2. The ozone RAF at 305 nm irradiance as a function of ozone and *sza*.

Figure 3 shows 305 nm irradiance measurements in Sodankylä from the period of 1990- 2000. Only the snow-free conditions are included and the measurements are corrected for the Earth-Sun distance. The measurements performed at *sza* range 63-65 degrees are selected. In the left y-axis is irradiance at 305 nm, while in the right y-axis are the estimated ozone RAFs.

If a relationship between clear-sky irradiance and ozone amount existed, one could estimate the ozone dependent RAF. If this relationship was exactly log-linear, there would be a single RAF for any ozone. However, this is not the case for global irradiance (direct+diffuse), therefore the ozone RAF depends on ozone amount as well. Our procedure to estimate the clear-sky irradiance against ozone is similar to *Fioletov et al.* [1997], who developed a parameterization for clear-sky irradiance at 324 nm as a function of *sza*. In brief, it is based on 95% percentiles at 40 DU steps of ozone amount. Finally, a third-order polynomial is fitted into these clear-sky estimates at 40 DU classes. The parameterization is plotted as a blue line in the figure and the corresponding ozone RAF is plotted in pink. The green line of ozone RAF is based on radiative transfer model, i.e. from the Figure 1 at a single *sza*. Evidently, it is difficult to derive a good estimate for the ozone RAF that depends on the ozone amount. The one based on measurements is lower than the model-derived estimate for most of the ozone values, until it increases rapidly at ozone amounts greater than 360 DU. On the other hand, there are less data at high ozone amounts and in turn the estimate of clear-sky irradiance is less accurate.

Figure 4 shows similar analysis to the data of Thessaloniki, the range of *sza* is from 49 to 51 degrees. Thus the RAFs are lower if compared to the previous figure. Again, the estimate from the measurements is lower than the model-derived values. Although it is not straightforward to provide very accurate estimates for the

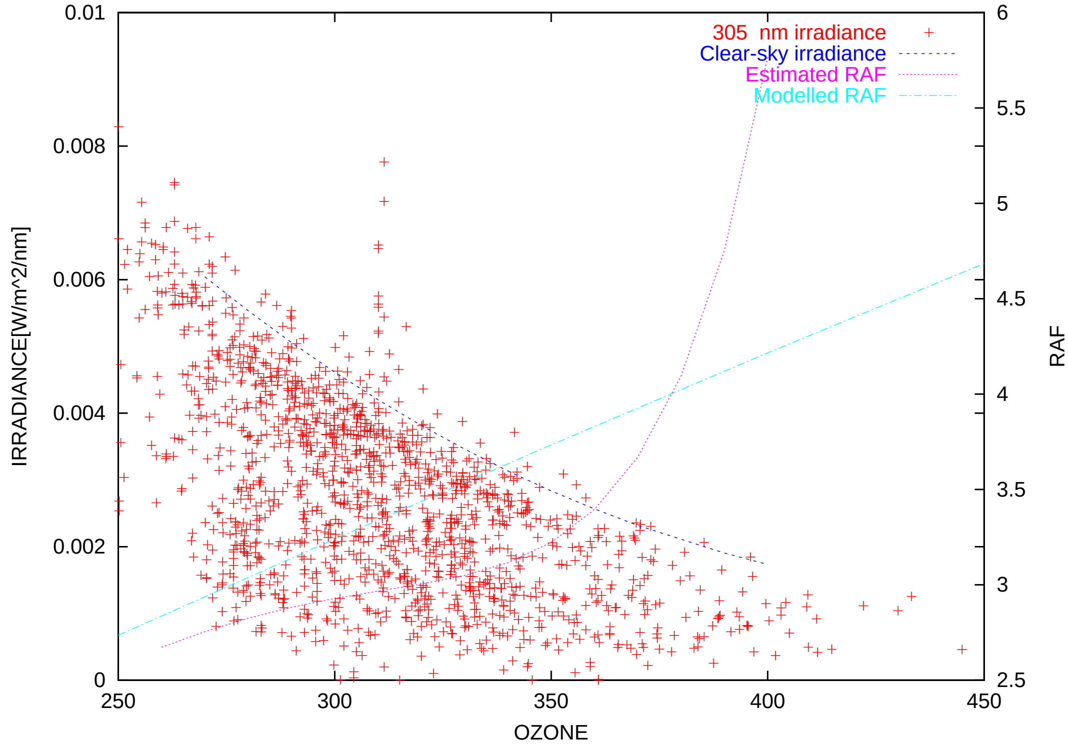

Figure 3. The 305 nm irradiance measurements at *sza* range of 63-65 in Sodankylä. Clear-sky irradiance (blue line) is estimated from the measurements. The ozone dependent ozone RAF is estimated from the radiative transfer model and from the spectral measurements.

ozone dependent RAF, deduced from the measurements, quantitatively in both cases the measurements indicated similar dependency than the model estimates.

3. Albedo RAF

3.1. Background on the snow impact in UV

There exist some previous studies, in which the enhancement in UV due to the snow have been investigated. *McKenzie et al.* [1998] reported from the data of case study that UV-B increased due to the snow by about 30% under clear sky and about 70% under cloudy sky at Lauder, New Zealand. *Weihs et al.* [1999] observed enhancement of 15-20% in Sonnblick Observatory, Austria. Comparing Brewer measurements with and without snow, *Fioletov and Evans* [1997] showed that on average snow enhances clear-sky flux at 324 nm by 39% at Churchill, by 21% at Edmonton and by 12% at Toronto. *Kylling and Mayer* [2001] compared 340 nm irradiance fluxes to the snow-free conditions, moving the snowline from 0 to 1000 m.a.s.l. around Tromsø . For a cloudless sky enhancement of 23-27% was achieved, while for overcast conditions the enhancement was 40-60%. Recently, *Smolskaia et al.* [2003] analyzed the data of a measurement campaign, carried out at French Alps. Erythemal irradiance enhancement due to the snow was about 5-15% and as high as 22% after the snowfall.

Albedo RAF, defined similarly to ozone RAF, cannot be estimated from the data measurement-by-measurement basis. However, an equation can be derived to relate the change in surface albedo to the change in irradiance. This derivation can be found from e.g. *Lenoble* [1998] and it results in the following geometric series.

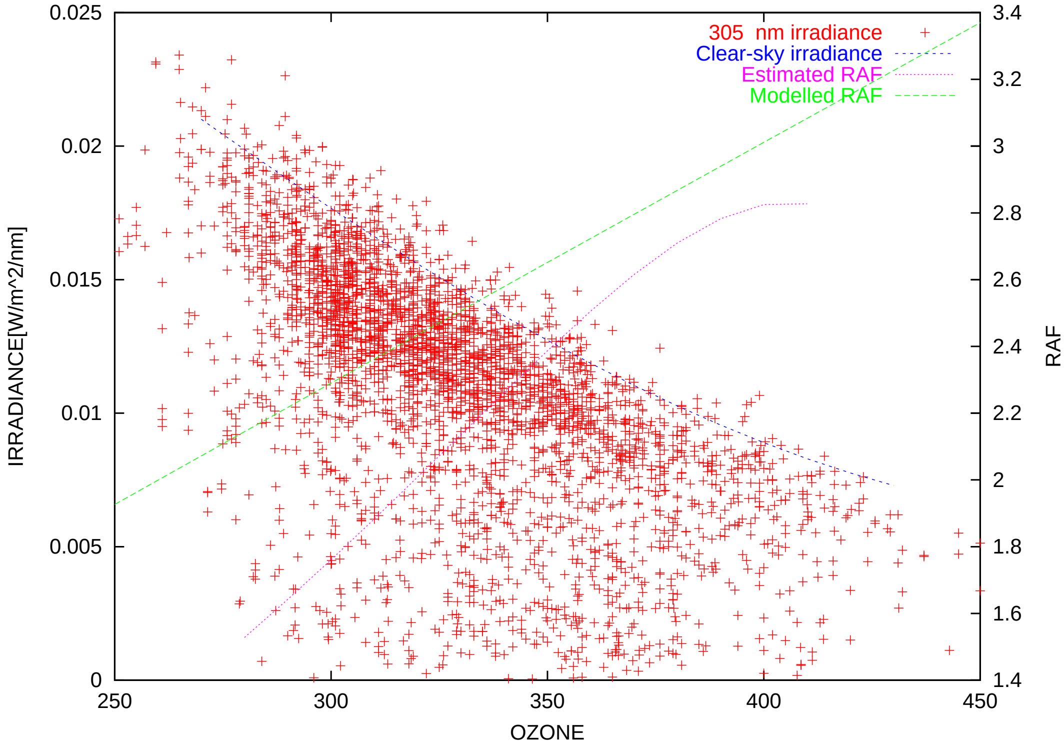

Figure 4. The 305 nm irradiance measurements at *sza* range of 49-51 in Thessaloniki. Clear-sky irradiance (blue line) is estimated from the spectral measurements. The ozone dependent ozone RAF is estimated from the radiative transfer model and from the spectral measurements.

$$RAF = \frac{1}{1 - S * A}, \tag{1}$$

where now RAF stands for the albedo RAF, S is the atmospheric reflectance and A is the surface albedo. The equation gives the irradiance enhancement due to the albedo of A, relative to the zero albedo. Evidently, albedo RAF is more complex than ozone RAF. The atmospheric reflectance should be known, which in turn depends on the state of the atmosphere. Moreover, albedo is not a trivial parameter to be determined. It depends on the effective area and its homogeneity. If we are interested in the albedo for spectral UV measurements, the effective area is different if compared to the albedo estimate derived from pyranometer measurements of reflected and global measurements. In the latter case, it is based on measurements affected typically by small and unbroken area, whereas spectral measurements during snow-cover may be affected by an area of 40 km (*Degünther et al.* [1998]). A normal way to determine the effective albedo is to compare the measurements during snow-covered and snow-free conditions to estimate how much the irradiance in some location is increased by the snow. However, this enhancement is precisely the RAF in the equation 1. Thus the problem of albedo RAF becomes "which came first chicken or egg" type of situation; in this case "which came first Albedo RAF or Albedo"?

One of the complications in the definition of albedo RAF is that the atmospheric reflectance should be known. Figure 5 shows the reflectance as a function of wavelength for three different conditions. First aerosol-free atmosphere is shown with two ozone amounts and third (blue) line is with absorbing aerosols. The specific amount of aerosols is not important here, the purpose of the figure is simply to illustrate the fact that the snow enhancement is a complex function of the state of the atmosphere. First the reflectance increases with decreasing wavelength, due to the Rayleigh scattering and below around 320 nm decreases due to the ozone absorption.

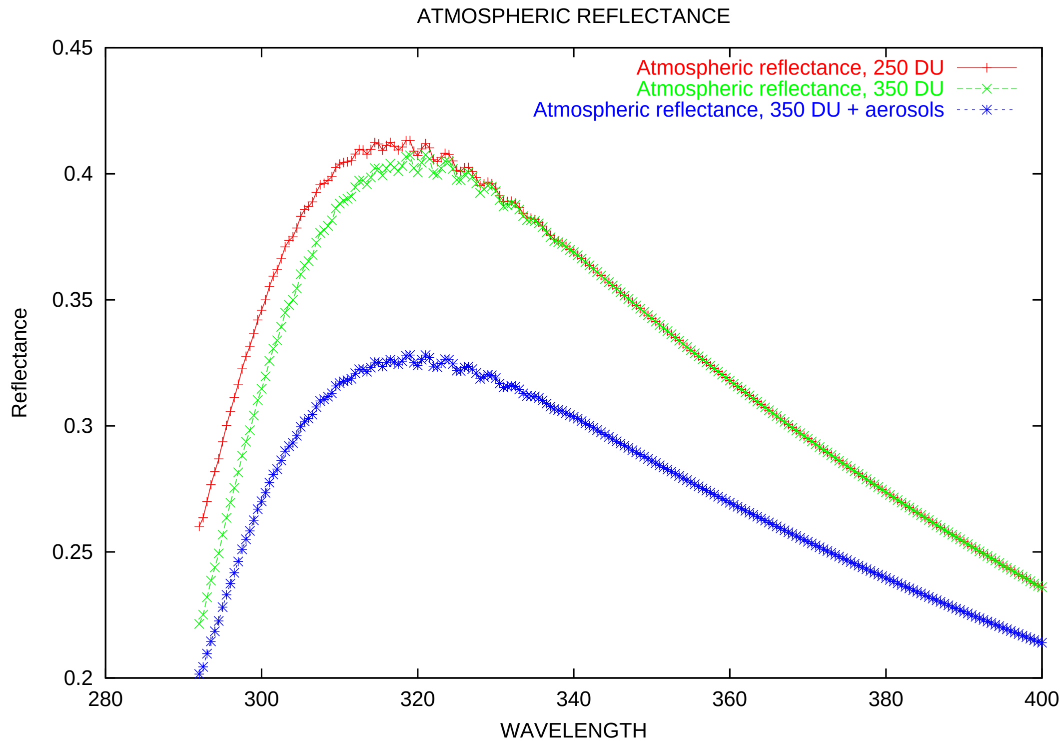

Figure 5. The atmospheric reflectance as a function of wavelength.

The albedo itself is not a trivial measure and depends on the effective area influencing the measurement used to derived it. Figure 6 shows a scatter plot of two albedo estimates, both in Sodankylä. In y-axis is shown the ratio of reflected to global irradiance, measured by the pyranometer in Sodankylä. The reflected component is measured by downwards pointing instrument, so the influencing area is rather small. On the other hand, in x-axis is corresponding albedo that is based on TOMS 380 nm reflectivity measurements when according to the actual SYNOP measurement in Sodankylä there was cloud-free and snow-covered conditions. Moreover, a relationship was found between clear-sky TOMS measurement and measured snow depth. This is based on gridded TOMS product of 1x1.25 degrees, so it can include very heterogeneous surfaces. This methodology follows the idea of [A. Arola et al., manuscript submitted to JGR, 2003], who developed a snow albedo algorithm for satellite UV retrieval method. The measurements are typically between 0.5 and 0.6, while the albedo estimate from the pyranometer measurements is systematically larger. In the next section it will be shown that the estimate for the average snow surface albedo, estimated from the Brewer measurements, is about 0.4. Therefore, all these three approaches to estimate the albedo result in different values, which is mostly explained by the differences in the effective area.

Figure 7 shows a model simulation of albedo RAF against wavelength for four different albedo values. Based on the equation 1 it shows the ratio of global irradiance with the given surface albedo to the irradiance with zero surface albedo, assuming in this simulation aerosol- and cloud-free atmosphere.

Since the albedo RAF, which would be similar to ozone RAF, cannot be determined measurement-by-measurement basis, in this WP snow effects on surface UV have been studied in two different ways. First, the enhancement due to the snow, i.e. albedo RAF on average sense, is calculated from the Sodankylä data for both clear-sky and

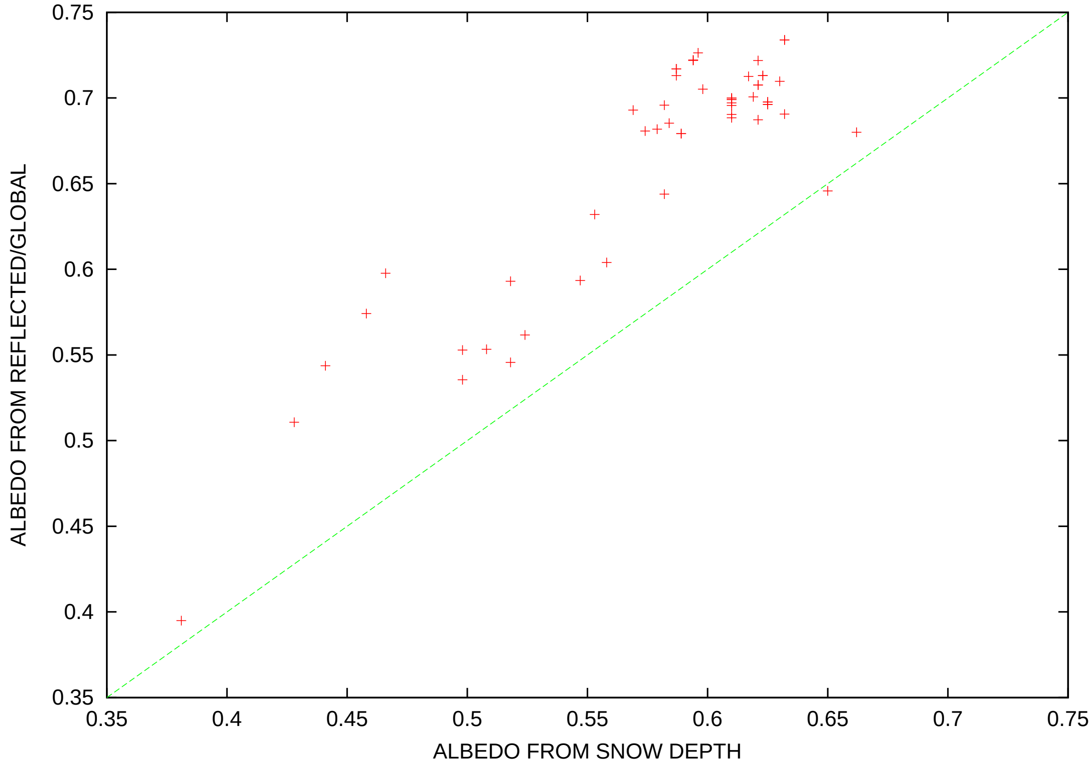

Figure 6. Albedo determined from pyranometer measurements (y-axis) and from the TOMS 380 nm reflectivity measurements (x-axis).

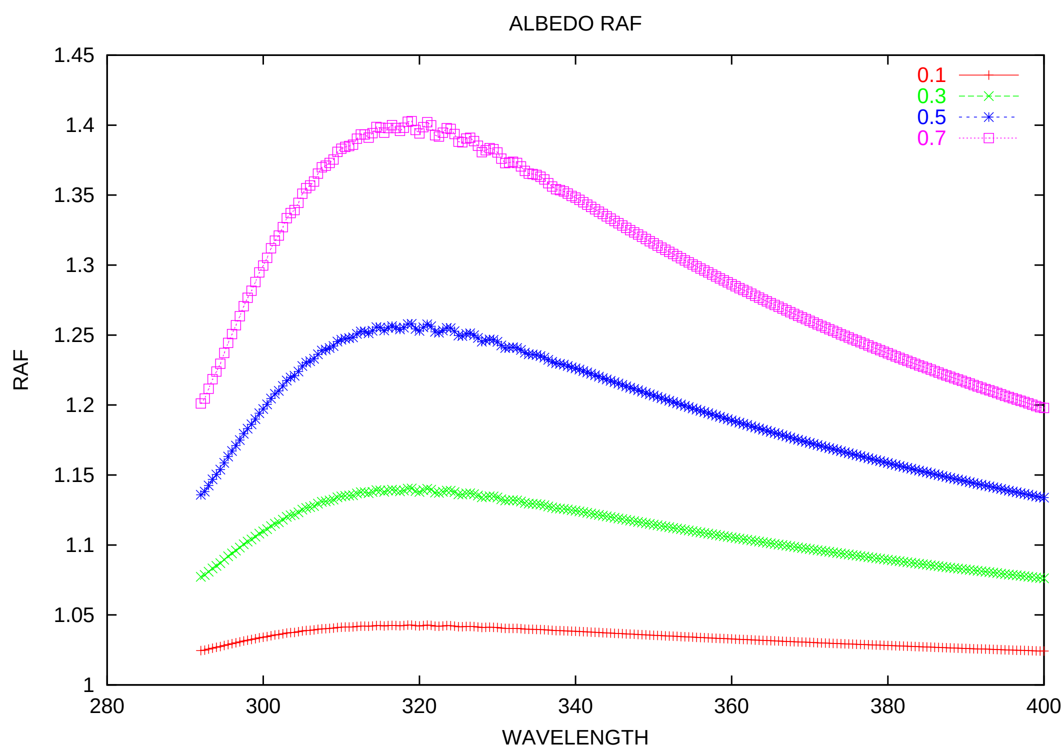

Figure 7. The albedo RAF at 305 nm as a function of wavelength.

overcast conditions. Second, ozone and albedo impacts (relative to the climatological conditions) on surface UV are estimated. Both of these approaches are described below in separate sections.

3.2. Average albedo RAF at clear-sky and overcast conditions

Figure 8 shows all 324 nm measurements (at *sza* range of 63-65 degrees) from 11-year period at Sodankylä, when according to the SYNOP observations total cloudiness had been zero before and after the scan. In other words, clear-sky spectra are selected. On the x-axis is shown snow albedo estimated from the snow depth. It is based on TOMS reflectivity measurements as discussed before. However, in this context the actual albedo values are not important, while here the main point is to use the snow depth (or equivalently the snow albedo in x-axis) only to separate the measurements into two cases; those with snow on the ground and to those with snow-free conditions. For both cases, the mean irradiance is shown in the bottom of the figure. For instance, the mean irradiance in snow-free conditions is 0.00223, whereas during snow conditions it is 0.002659. Then the ratio of snow to snow-free mean irradiance tells us how much snow increases the irradiance. This ratio is the average albedo RAF, as defined in the equation 1. In other words, the average snow enhancement in Sodankylä is 1.19 or 19%. If a realistic value for the atmospheric reflectance is assumed, which is around 324 nm for a rather clean atmosphere about 0.4, an estimate for average albedo of 0.4 is resulted.

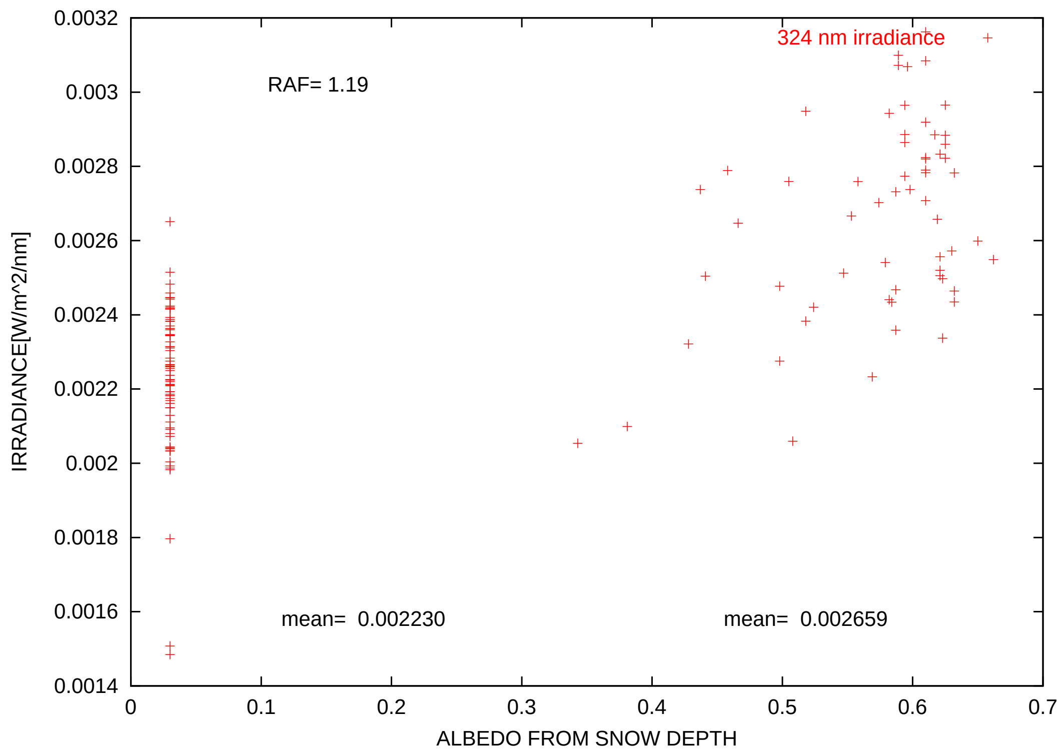

Figure 8. The irradiance measurements at 324 nm during clear-sky conditions.

The next figure (Figure 9) shows exactly similar analysis, but now only those measurements are included that have had total cloudiness of 8 octas before and after the scan. Now the data are very scattered, since the total cloudiness alone is not a good indicator of the cloud optical properties. However, in the average sense the snow enhancement can be estimated. Now the albedo RAF during overcast conditions is higher (about 70%) due to the interaction between surface and clouds, i.e. the atmospheric reflectance in the equation 1 is increased due to the clouds.

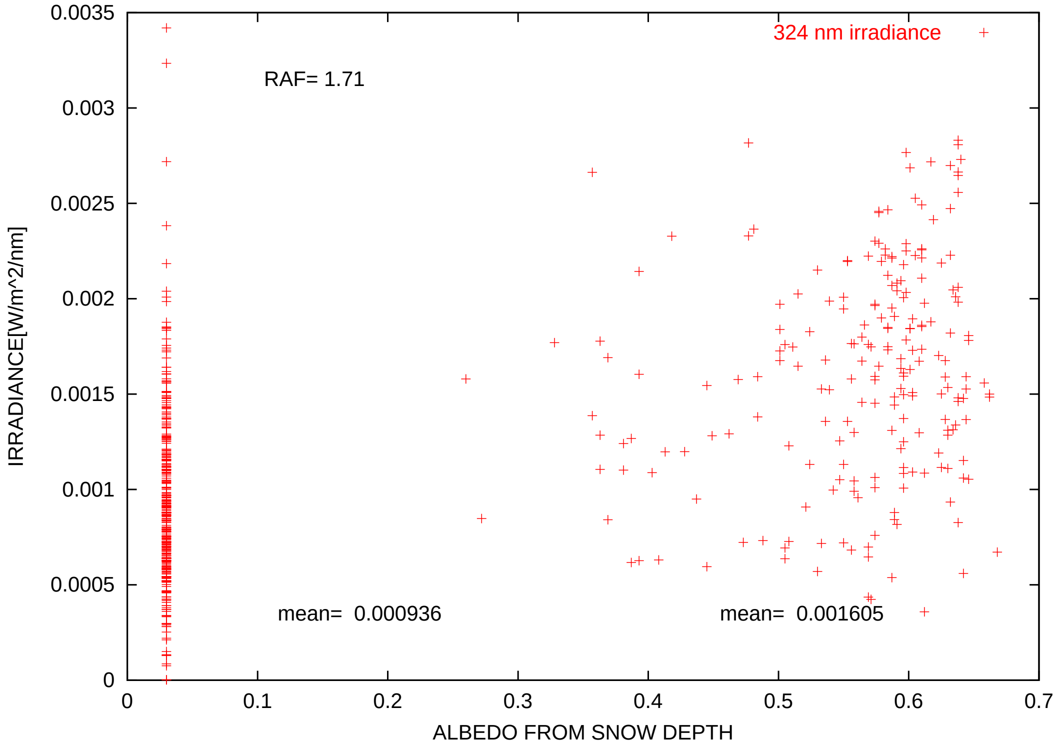

Figure 9. The irradiance measurements at 324 nm during overcast conditions.

3.3. UV variability induced by the snow surface

In this section, the results of ozone and albedo influences in the surface UV, compared to the average conditions (to the daily climatology), are presented. The approach to produce the irradiance time series affected only by a given factor has been described in detail in the final report of the WP 2.1. This same approach is now applied and the spectral measurements selected for the analysis were simulated for the entire 11-year period with different input data combinations. The necessary input variables to reconstruct the measurement can be denoted by $(O_3, \alpha, \tau_a, \tau_c)$, where the input data of ozone, surface albedo, aerosol optical depth and cloud optical depth for each irradiance measurement are formed as described in the final report of WP 2.1. Similarly, the input data needed to estimate the irradiance from the daily climatologies are denoted by $(\overline{O_3}, \overline{\alpha}, \overline{\tau_a}, \overline{\tau_c})$, where a line over a variable refers to the climatology. Thus, the combination of $(O_3, \overline{\alpha}, \overline{\tau_a}, \overline{\tau_c})$ consistently produces irradiance time series that is affected only by the actual ozone variability, while the other input variables follow their daily climatology. The daily climatology of each input variable was estimated from the 11-year data. For instance, for ozone the daily climatology value on day 130 was calculated as the average of the ozone measurements on day 130 from 1990 to 2000. Moreover, a 5-day moving-average filter was applied to smooth out the strongest short-term variations.

Figure 10 shows the results for 305 nm in April. The ozone run (red) is generated with the input set of $(O_3, \overline{\alpha}, \overline{\tau_a}, \overline{\tau_c})$, while for the albedo run (blue) the set of $(\overline{O_3}, \alpha, \overline{\tau_a}, \overline{\tau_c})$ is used. On the y-axis they are shown relative to the daily climatology. For instance, on this axis, the ozone run is the ratio of simulations with the data sets of $(O_3, \overline{\alpha}, \overline{\tau_a}, \overline{\tau_c})$ and $(\overline{O_3}, \overline{\alpha}, \overline{\tau_a}, \overline{\tau_c})$. In the upper left corner of the figure some statistics are shown. The amplitude of each factor is calculated as (maximum-minimum)/mean of the ratios of the entire data, indicating the maximum possible variability induced by each factor, while the standard deviation gives a measure of the variability on average sense. In this analysis, every single measurement is included, whereas the corresponding values in parentheses are calculated from the monthly mean irradiance data. It is noted that the x-axis is not a strict time axis. Ozone time series is advanced by a lag of 70 days, simply to separate it from the corresponding albedo data and to better illustrate the differences between them. If a strict time axis was used, they would overlap, since they are based on same irradiance measurements in April.

It can be seen that the ozone-induced variability in April is much stronger than the surface albedo effect. In the 305 nm irradiance measurements in April, a variability of almost 280% can be caused by ozone, while in an average sense it is about 50%. In monthly mean irradiances the corresponding values are 93% and 35%, respectively. By comparison, the variability in the 305 nm flux caused by the albedo effect is on average 3% in monthly levels, being about at most 9%.

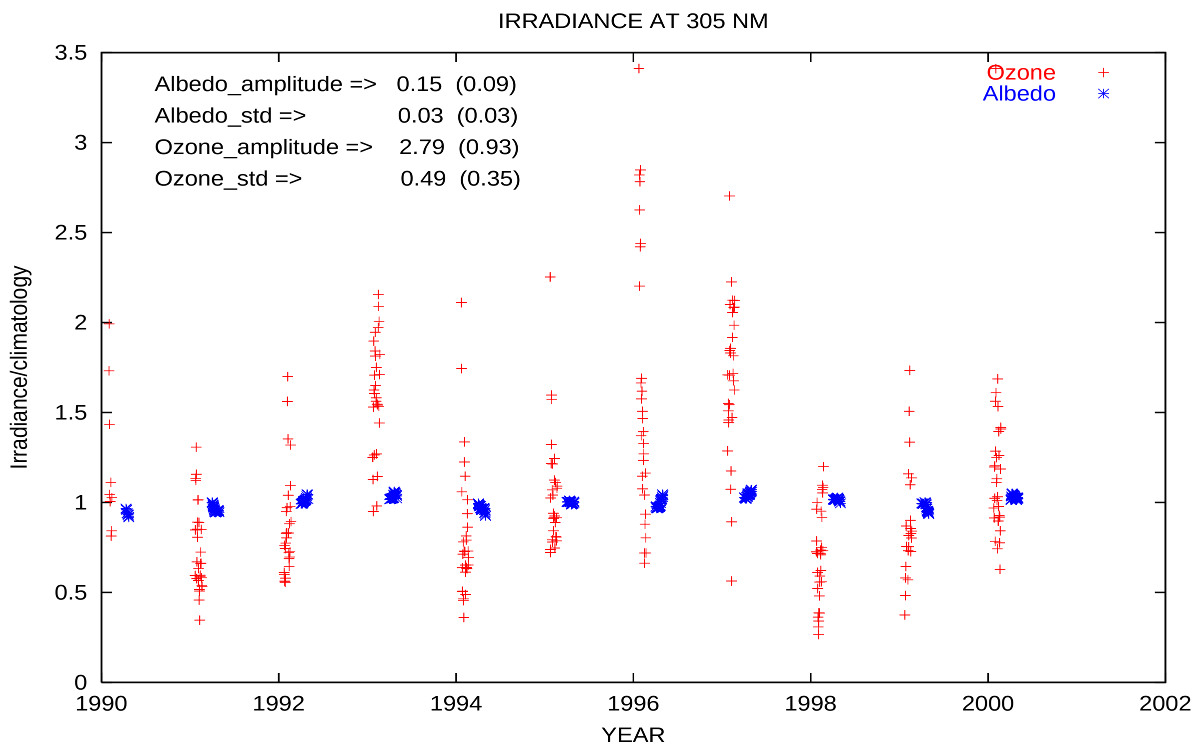

Figure 10. The effect of ozone and albedo on UV variability in April. The y-axis values are the ratios of the simulations to the values of the climatological input data set.

Figure 11 is otherwise similar to the Figure 10, but now the results for May are presented. It is evident that the albedo effect is much stronger. At Sodankylä snow melts typically during May, but there can be a temporal variability of several weeks. The albedo, therefore, has its strongest effect in May, and can induce a variability of over 21% in monthly mean irradiance (about 7% on average). This effect is further enhanced at 324 nm, where it is about 26% (not shown), in accordance with the wavelength-dependent amplification of irradiance due to the snow (e.g. *Lenoble* [1998]).

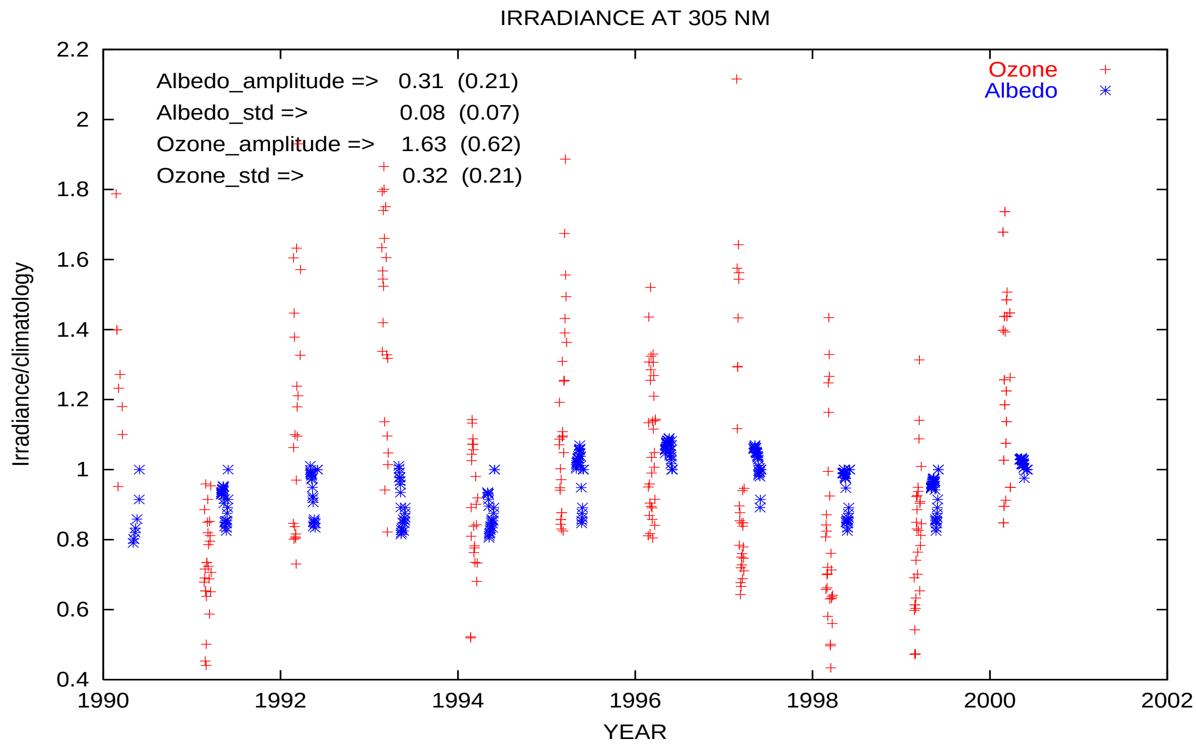

Figure 11. Otherwise similar to the Figure 10, but the results of May are presented

All the data combinations for both sites were simulated; only the most prominent cases have been discussed above. The findings can be summarized by concluding that in spring ozone has clearly the biggest influence on the UV. It can be noted also that the average variability, caused by the snow albedo changes, is basically the same regardless of whether the entire data set or monthly means are considered, while ozone causes more rapid short-term variability. In general our results agree with *Kylling et al.* [2000], who analyzed data from Tromsø and concluded that snow can increase the doses by 20%. However, it should be emphasized that these studies are not equivalent in their approach. *Kylling et al.* [2000] used one year's data only, but more importantly, they compared the changes to the snow-free or cloud-free cases. Our intention has been to compare the changes to the daily climatology, i.e. to the average conditions.

4. Conclusions

The main results can be summarized as follows:

1) Ozone RAF it is not only a function of *sza*, but also a function of ozone. However, this dependency has not been estimated previously from the measurements. Therefore, an attempt was made in this WP 1.4. From both data of both Sodankylä and Thessaloniki, ozone dependency was found that qualitatively agrees with model simulations.

2) Average clear-sky albedo RAF in Sodankylä is about 20%, estimated from the enhancement by snow if compared to the snow-free conditions.

3) Albedo RAF during overcast conditions was in average 70%

4) If the effects of ozone and snow albedo are considered in the variability in monthly mean irradiance at 305 nm, ozone plays clearly the biggest role. In monthly mean irradiances ozone impact is on average 35%, but can have an effect as high as 93%, while the albedo induced variability is about 7% and 21%, respectively.

References

Bais, A., C. Zerefos, C. Meleti, I. Ziomas, and K. Tourpali, Spectral measurements of solar radiation and its relation to total ozone, SO_2 and clouds, *J. Geophys. Res.*, *98*, 5199–5204, 1993.

Degünther, M., R. Meerkötter, A. Albold, and G. Seckmeyer, Case study on the influence of inhomogeneous surface albedo on uv irradiance, *Geophys. Res. Lett.*, pp. 3587–3590, 1998.

Fioletov, V., and W. Evans, The influence of ozone and other factors on surface radiation, in *Ozone science: A Canadian Perspective on the Changing Ozone layer*, edited by D. Wardle, J. Kerr, C. McElroy, and D. Francis, pp. 73–88, Environment Canada, 1997.

Fioletov, V., J. Kerr, and D. Wardle, The relationship between total ozone and spectral UV irradiance from Brewer observations and its use for derivation of total ozone from UV measurements, *Geophys. Res. Lett.*, *24*, 2997–3000, 1997.

Kylling, A., and B. Mayer, Ultraviolet radiation in partly snow covered terrain: Observations and three-dimensional simulations, *Geophys. Res. Lett.*, *28*, 3665–3668, 2001.

Kylling, A., A. Dahlback, and B. Mayer, The effect of clouds and surface albedo on UV irradiances at a high latitude site, *Geophys. Res. Lett.*, *27*, 1411–1414, 2000.

Lenoble, J., Modeling of the influence of snow reflectance on ultraviolet irradiance for cloudless sky, *Appl. Opt.*, *37*, 2441–2447, 1998.

Madronich, S., UV radiation in the natural and perturbed atmosphere, in *UV-B radiation and ozone depletion: Effects on Human, Animals, Plants, Microorganisms, and Materials*, edited by M. Tevini, pp. 17–69, Lewis Publishers, 1993.

McKenzie, R. L., K. J. Paulin, and S. Madronich, Effects of snow cover on UV irradiance and surface albedo: A case study, *J. Geophys. Res.*, *103*, 28,785–28,792, 1998.

Smolskaia, I., D. Masserot, J. Lenoble, C. Brogniez, and A. de la Casiniere, Retrieval of the ultraviolet effective snow albedo during 1998 winter campaign in the French Alps, *Appl. Opt.*, *42*, 1583–1587, 2003.

Weihs, P., S. Simic, W. Laube, W. Mikielewicz, G. Regarajan, and M. Mandl, Albedo influences on surface UV irradiance at the Sonnblick high mountain Observatory (3106 m altitude), *J. of App. Meteorology*, *38*, 1599–1610, 1999.

WMO, *Scientific Assessment of Ozone Depletion: 2002*, World Meteorol. Organ., Geneva, 2002.